

# Surface Roughness Investigation On Metal Spinning Components Applying Image Processing Approach

Dr. S. Gajanana<sup>1</sup>, Dr. B. Ravi Kumar<sup>1</sup>, Ravva Pavan Uttej<sup>1</sup>, Tejaswi Dittakavi<sup>1</sup>, Mohd Abdul Moid<sup>1</sup>,  
Pavan Chaitanya<sup>1</sup>

<sup>1</sup> Department of Mechanical Engineering , Maturi Venkata Subba Rao (MVSR) Engineering College, Telangana,  
Hyderabad, India

\*\*\*

**Abstract** - Metal spinning is forming of ductile materials into seamless axisymmetric components by combination of rotational motion and force. Metal spinning can be used to cost effectively produce a small number of parts out of expensive materials or large quantities of components of low-cost materials such as aluminum reflectors. In manual spinning, a circular blank of flat sheet is pressed against a rotating mandrel using a rigid tool. The tool is moved manually over the mandrel to form the component. It is reported that during deformation the work piece stretches in the radial direction and compresses circumferentially aiming to keep the original wall thickness constant. The surface finish of spun component is usually of sufficient quality that no additional machining is required after spinning. The surface finish of spun component is typical of 1.5-micron order. In this work on conventional metal spinning of Al2024 metal by three different rollers namely single roller, double roller, and double radii roller are used to obtain cylindrical profile components. The surface roughness of finished product is measured by Talysurf which are formed at three different speeds on three different thickness of sheets. The present study is to explore adaptivity of non-contact measurement of roughness by using Image Processing. The study reveals that the Image Processing method can be adopted with considerable error. The surface roughness has significant in functional applications of spun parts.

**Key Words:** Cylindrical profile, Image processing, Roller tool, Surface roughness, Thickness of sheet

## 1. INTRODUCTION

Spinning is a severe cold working operation where in a well-defined and directional grain flow pattern is produced which makes tensile and yield strength increase and ductility decrease. The magnitude of this depends on an amount of wall thickness reduction and on susceptibility of metal to work hardening. The initial position and path of roller is the key parameters in cone spinning. In majority of cases the shape, dimensional accuracy and surface finish of spun parts, the stability of tool forces in the process are the most useful criteria in spinning process design and production. [1] For conventional spinning process, it involves many random process parameters such as variation of material flow stress, initial thickness, profile of roller path, geometry of roller,

roller feed rate and frictional condition between workpiece and tool: [2] The Authors reported that the relative stress patterns are identical trend for various thickness of the sheets. According to Hayama low mandrel speed, smaller diameter of roller and low viscosity lubricant give low surface finish [3]. Roller nose radius also has the significant effect on dimensional accuracy, the larger nose radius resulted in uniform thickness and low surface roughness. Sandeep Kamboj et al., concluded that the variation in feed ratio has a considerable effect on tool forces, spinnability and surface finish [4]. A high feed ratio results into higher forming force and lower feed ratio results in excessive material flow in the outward direction which results a better surface finish without the failure of the material. The researchers concluded that the surface morphologies in cylindrical path are more uniform compared to radius R10 surface. Also reported that the surface roughness in the radius R10 region is higher compared cylindrical parts. The process of conventional spinning is investigated by many researchers, and it is still highly depending on spinner experiences. J.M Allwood mentioned the spinning process is used to produce components in symmetrical in axial direction, these components are used by several industries like automobile, aerospace, energy generation plants etc. [5] Surface roughness plays a key role in determining the quality of components, the components used by aerospace industry should have high surface finish so that stress failures reduce, production and manufacturing sectors also prefer to have higher surface finish especially for moving parts in engine so that the efficiency improves [6]. To develop a further understanding of the process, the experimentation is carried to evaluate the surface roughness by varying roller geometry. Image processing methodology is adopted to measure the roughness of the cylindrical parts with help of MATLAB software. In image processing method the cylindrical specimen pictures are taken in a digital camera, then its picture is transformed into binary form to measure the roughness value of the cylindrical part.

## 2. MATERIALS USED

### 2.1 Work Piece:

The experiment is carried out on Engine Lathe to obtain cylindrical profile. For an aluminium alloy 2024 which is

extensively used in aerospace and household utensils. The chemical composition of the workpiece is tabulated in table 1

### 2.2 Roller (Spinning tool)

Roller is used to apply force against the sheet metal, to form the component as per requirement. Dakshesh proposed as in order to get good surface finish one need to maintain the speed of Mandrel high and should use larger diameter roller. Roller radius determines the dimensional accuracy, with larger noise radius gives uniform thickness while spinning operation.[7]. The geometry of tools used for experimentation are single roller, double roller and double radii roller. The types of roller is illustrated in figure (1) and chemical composition of the roller is tabulated in table 2

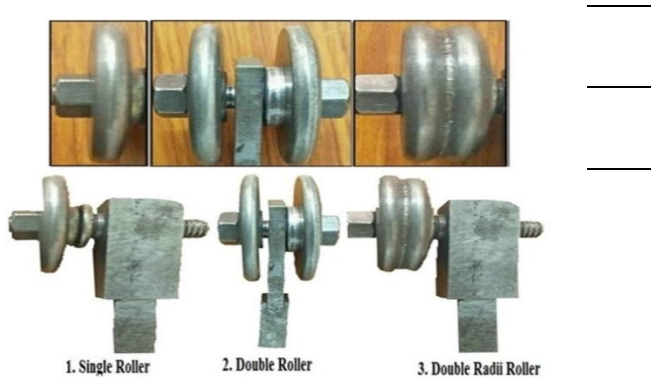


Table 1: The chemical composition of the specimen

Constituent material	Al	Cr	Cu	Fe	Mg	Mn	Si	Ti	Zn
Weighted percentage	90.7-90.1	0.1	3.8-4.9	0.5	1.2-1.8	0.3-0.9	0.5	0.15	0.25

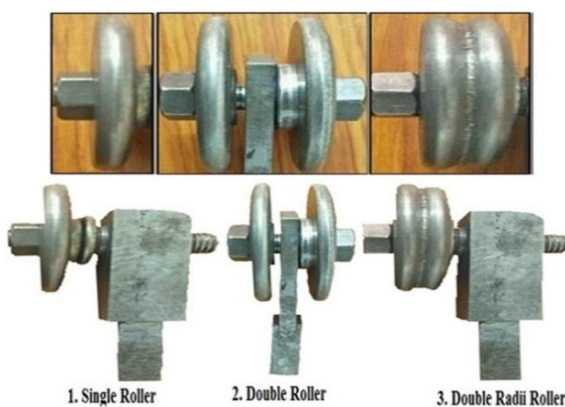


Figure 1: Type of Rollers

### 2.3 Mandrel

Mandrel determines the shape of final workpiece. In this experiment we use cylindrical Mandrel. The diameter (d) of mandrel is taken as 50mm, the blank size (S) is taken as 85mm × 85mm as reference. The height (h) is calculated by the equation 1, the mandrel 2-d design is illustrated in the figure (2)

$$S \times S = \pi d \left( \frac{d}{A} + h \right) \tag{1}$$

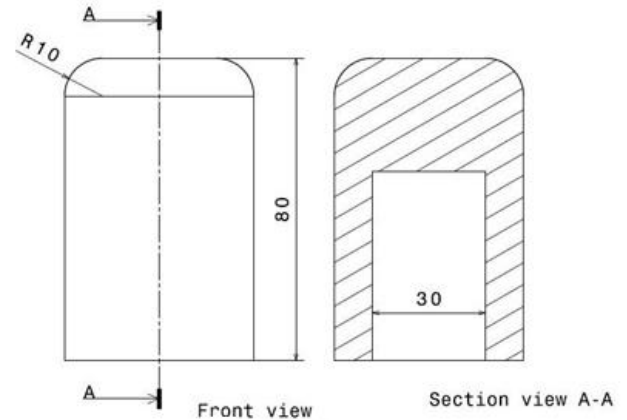


Figure 2: Mandrel 2-d sketch

Table 2: The chemical composition of roller

Constituent member	C	Mn	Si	S	P
Percentage	0.35-0.40	0.60-1.00	0.10-0.40	0.50	0.50

### 3 EXPERIMENTATION

The following input settings were used in an independent experiment on a cylindrical component using the Taguchi L9 array: 1 mm sheet thickness, 133 rpm mandrel speed, and a single roller spinning tool. By adjusting the speed between 133 and 207 rpm, the sheet thickness between 1 and 1.5 mm, and with three distinct roller types—Single roller, Double roller, and Double radii roller—the viable space for the spinning parameters was identified. Three levels of the parameters were chosen for the spinning parameter design. Surface roughness is the output parameter taken into consideration for study. Table 3 displays the numerous input variables utilized in the experiment and design matrix for experimentation as per Taguchi is illustrated in table 4. Fig. 3 and Fig. 4 show the experimental setup and spur components. Using the Mitutoyo Surf-test indicator, the surface roughness is calculated, and the values are shown in Table 5 for various experimental trials.

**Table 3:** Metal spinning factors and levels

Factors	Units	Test levels		
		Level 1	Level 2	Level 3
Speed	Rpm	133	150	207
Thickness of sheet	Mm	1	1.2	1.5
Roller type	-	Single roller	Double roller	Doble radii roller

**Table 4:** Design matrix for experimentation

Experiment no	1	2	3	4	5	6	7	8	9
Speed	1	1	1	2	2	2	3	3	3
Sheet Thickness	1	2	3	1	2	3	1	2	3
Roller type	1	2	3	2	3	1	3	1	2



**Figure 3:** Experimental setup



**Figure 4:** Specimen Components

The standard deviation, which is determined to give a sense of the precision of the data, is calculated and is found to be 0.14  $\mu\text{m}$  from taking values of table 5. Figure 5 illustrates the specimen's pattern of surface roughness. Experimental data show an average roughness of 0.52  $\mu\text{m}$ .

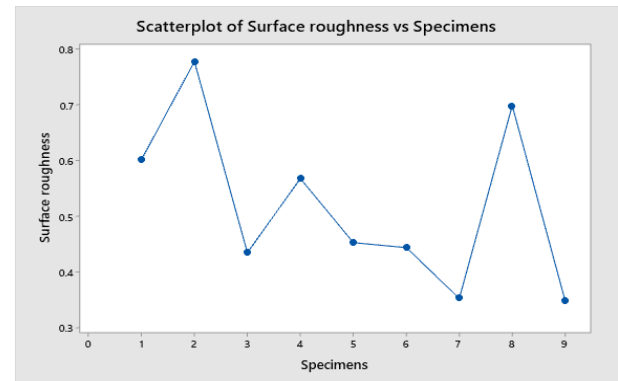


**Figure 5:** Graph of experimental surface roughness values

**Table 5:** Experimental Result

S.No	Speed	Thickness	Roller Type	Surface Roughness
	S (rpm)	T (mm)	R	SR ( $\mu\text{m}$ )
1	133	1	1	0.602
2	133	1.2	2	0.778
3	133	1.5	3	0.435
4	150	1	2	0.568
5	150	1.2	3	0.453
6	150	1.5	1	0.444
7	207	1	3	0.353
8	207	1.2	1	0.699
9	207	1.5	2	0.348

#### 4 Image processing

Prior to image processing, cylindrical specimen photographs are obtained with a digital camera that is positioned 90 degrees from the specimen. All of the specimens are separated into eight equal pieces, each of which is photographed using a digital camera. All additional specimens are photographed using the same camera and lighting source. Then, MATLAB is used to process the images for the purpose of assessing surface roughness. The following are the image processing methodologies

1. Converting RGB image into gray image
2. Normalization of gray image
3. gray image into binary image
4. finding RMS values from binary image matrix

### 4.1 RGB image to Gray image -

The rgb2gray function is used to convert a truecolor image to a grayscale image. By removing the hue and saturation data while keeping the brightness. Figure (6) and figure (7) indicates color image and gray scale image of the specimen 1 at 0°.

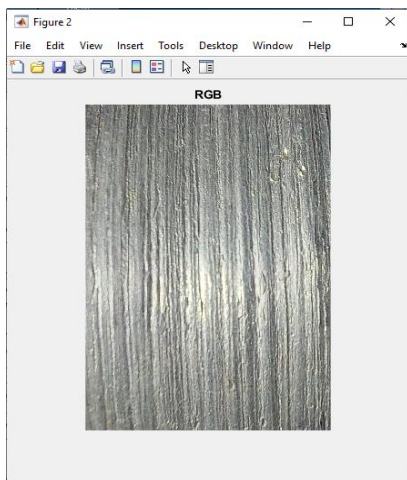


Figure 7: Gray image

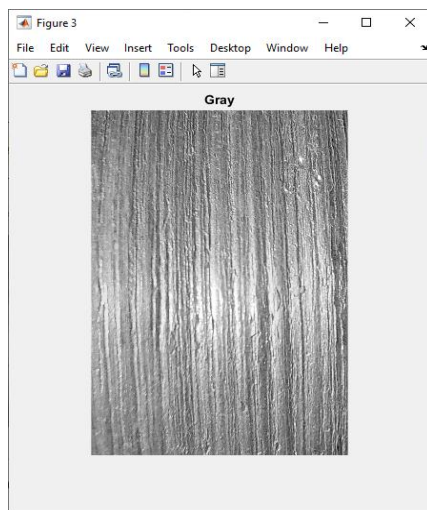


Figure 7: Gray image

### 4.2 Normalization of gray image -

Image normalization plays a key role in reducing the disturbances due to light source. Image normalization reduces lighting variation. Image normalization of gray image is done by using equation (2)

$$h(x, y) = \frac{k(x, y) - \min(k)}{\max(k) - \min(k)} \quad (2)$$

$h(x, y)$  is normalized matrix for the image matrix,  $k(x, y)$  is image matrix,  $\min(k)$  is minimum value of image matrix and  $\max(k)$  is maximum value of image matrix. Figure(8) represents normalized image of specimen 1 at 0°.

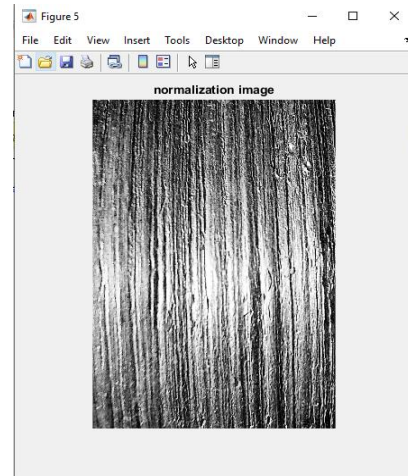


Figure 8: Normalized image

### 4.3 Binary matrix of image and calculations

The normalized matrix is then transformed into binary matrix form. Where it contains only 1 and 0. 1 is brightest and 0 is darkest pixel of image. The RMS values of image is calculated by using the binary matrix of image. Figure (9) is binary image of the specimen 1 at 0°, which is changed from normalized image to binary image.

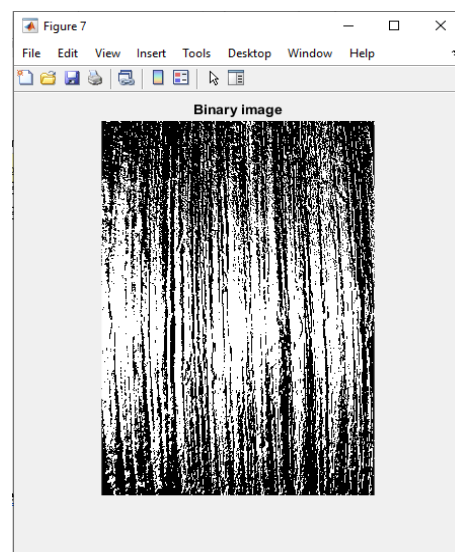
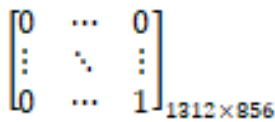


Figure 9: Binary image

**Table 6:** RMS values of specimens by using Image Processing

Angular Position	Specimen 1	Specimen 2	Specimen 3	Specimen 4	Specimen 5	Specimen 6	Specimen 7	Specimen 8	Specimen 9
0	0.5775	0.5773	0.5769	0.5771	0.5771	0.5776	0.5773	0.5770	0.5774
45	0.5776	0.5776	0.5776	0.5774	0.5772	0.5777	0.5771	0.5772	0.5766
90	0.5772	0.5769	0.5771	0.5784	0.5778	0.5779	0.5770	0.5774	0.5772
135	0.5772	0.5773	0.5774	0.5776	0.5777	0.5774	0.5771	0.5771	0.5776
180	0.5775	0.5779	0.5774	0.5774	0.5771	0.5772	0.5778	0.5769	0.5771
225	0.5774	0.5770	0.5770	0.5773	0.5778	0.5774	0.5776	0.5771	0.5771
270	0.5771	0.7022	0.5774	0.5778	0.5776	0.5771	0.5771	0.5772	0.5769
315	0.5773	0.6947	0.5776	0.5773	0.5776	0.5775	0.5770	0.5774	0.5770
Average	0.57735	0.607613	0.5773	0.577538	0.577488	0.577475	0.57725	0.577163	0.577113



Binary matrix

From the values obtained by image processing the standard deviation is observed as 0.02  $\mu\text{m}$ . The average surface roughness is 0.58069  $\mu\text{m}$ . From the table 6 it is observed that the value of the surface roughness is minimal for the specimen 9 as the experimental result for surface roughness.

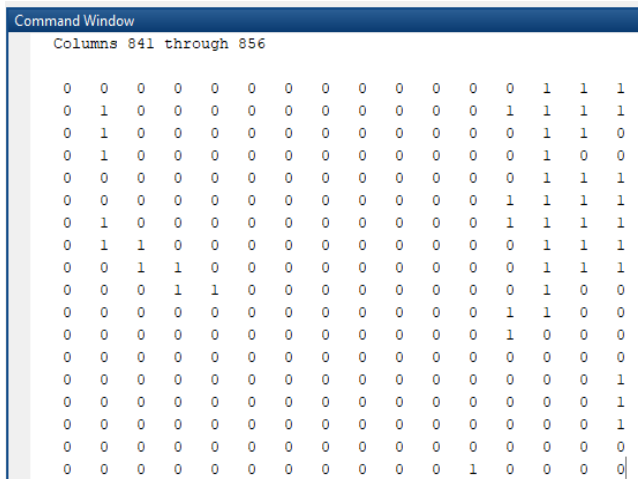


**Figure 10:** Binary matrix

Figure (10) represents the binary image pixel value for column 841 to 851 and up to 20 rows of specimen 1 at 0°.

In similar manner for remaining 8 specimens the binary matrix is prepared at different angular position of 45°, 90°, 135°, 180°, 225°, 270° and 315°. The RMS and Ra values are tabulated in the table 6

**Table 7:** Ra values of specimens by using Image Processing

Angular Position	Specimen 1	Specimen 2	Specimen 3	Specimen 4	Specimen 5	Specimen 6	Specimen 7	Specimen 8	Specimen 9
0	0.5042	0.5002	0.5007	0.4956	0.5006	0.5040	0.4990	0.5032	0.4996
45	0.5006	0.4963	0.4993	0.5047	0.4978	0.5022	0.5027	0.5035	0.4990
90	0.4959	0.4964	0.5034	0.5067	0.5023	0.4989	0.4985	0.5033	0.4965
135	0.4986	0.5012	0.4993	0.4977	0.4985	0.5001	0.5004	0.4989	0.4996
180	0.5038	0.5034	0.4999	0.4990	0.4959	0.4988	0.5005	0.5035	0.5024
225	0.4958	0.5007	0.5019	0.4956	0.4968	0.5009	0.4978	0.4993	0.4983
270	0.4984	0.5020	0.5044	0.4997	0.4976	0.5008	0.5017	0.5027	0.4985
315	0.4993	0.5014	0.4963	0.4956	0.5041	0.4983	0.4993	0.5017	0.4964
Average	0.499575	0.5002	0.50065	0.499325	0.4992	0.5005	0.499988	0.502013	0.498788

The standard deviation of the values from table 7 is 0.00264  $\mu\text{m}$ , the average value is 0.5  $\mu\text{m}$ . The least average value of surface roughness is obtained from specimen 9.

### 6 References

- [1] Shi, F., Long, H., Zhan, M. and Ou, H., 2014. Uncertainty analysis on process responses of conventional spinning using finite element method. *Structural and Multidisciplinary Optimization*, 49(5), pp.839-850.
- [2] B Ravikumar, Dr S Gajanana, Dr K. Hemachandra Reddy, M. Krishna Reddy (2019): "Experimental Investigation and Numerical Simulation of Metal Spinning on A12024 using a Cylindrical Mandrel". *International Journal of Research and Analytical Reviews*, Volume 06, Issue 1, January, 2019
- [3] Hayama M, Kudo H, Shinokura T: "Study of the Pass Schedule in Conventional Simple Spinning". *Bulletin of JSME*, 13, 1358-1365, 1970
- [4] Sandeep Kamboj , Bharat Atray , Neeraj Kumar : "Analysis The Effects Of Different Types Of Tool On Metal Spinning Process" *International Journal Of Research In Engineering And Technology* Volume: 03 Issue: 02 164-70, Feb-2014.
- [5] Music, O., Allwood, J. M., & Kawai, K. (2010). A review of the mechanics of Metal Spinning. *Journal of Materials Processing Technology*, 210(1), 3-23. <https://doi.org/10.1016/j.jmatprotec.2009.08.021>

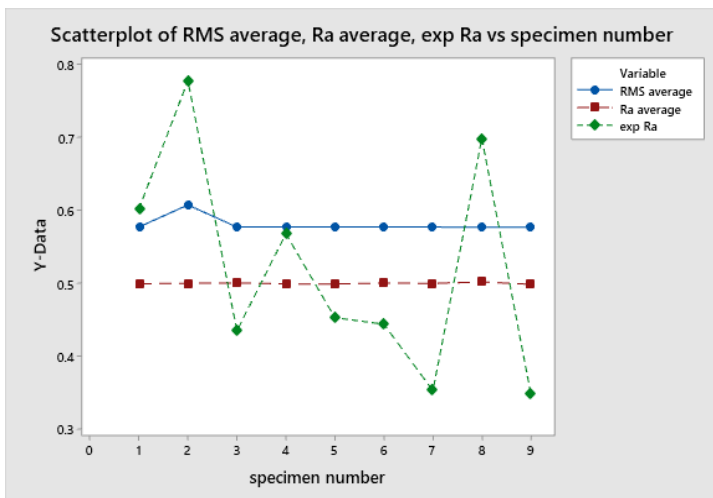


**Figure 11:** Comparison of values of experiment and Image processing values

### 5 Conclusion

The Rms value of binary image matrix is more adoptative than Ra value of the binary image matrix their values are more appropriate with the experiment values measured by Talysurf. The standard deviation of experimental values is closer to the RMS values of specimen using image processing. The surface roughness is found to be minimal for specimen 9 by both experimental result and by image processing method. Hence it is recent to adopt , the image processing can be used for measuring the surface roughness

- [6] Tennant, R. (1992), "Mechanical Surface Finishing in the Aerospace Industry", *Aircraft Engineering and Aerospace Technology*, Vol.64, No.3, pp.414. <https://doi.org/10.1108/eb037216>
- [7] Dakshesh Darji, Darshan Bhatt (2020). "Design and Investigation of spring loaded tool in metal spinning process in lathe", *journal of engineering sciences*, vol.11, Issue 6, June, 2020
- [8] Ali, Mahashar & . H, Siddhi Jailani & Murugan, M.. (2019). Surface Roughness Evaluation of Milled Surfaces by Image Processing of Speckle and White-Light Images. 10.1007/978-981-13-1724-8\_14.
- [9] Zhongxiang, H., Lei, Z., Jiaxu, T., Xuehong, M. and Xiaojun, S., 2009. Evaluation of three-dimensional surface roughness parameters based on digital image processing. *The International Journal of Advanced Manufacturing Technology*, 40(3-4), pp.342-348.